The Calculation Algorithm of the Informative Parameters of the Signal at Implementing the Method of Multiple Reflections

Yu. V. Myshkin, A. B. Efremov

Department of Instruments and Techniques for Measurement, Control, Diagnostics,
Kalashnikov Izhevsk State Technical University, Izhevsk, Russian Federation
E-mail: mubm@yandex.ru

Received: 30.11.2016

Abstract. The method of multiple reflections has several important informative parameters of the signal which allow to determine of the presence or the absence of defects in the testing object. Some parameters can be calculated using only numerical methods. In this article, the calculation algorithm of several key informative parameters of the signal is represented such as reflection coefficient on the interface "transducer – testing object", attenuation coefficient, probe pulse amplitude and position. Numerical values of informative parameters of the signal are obtained for pipes with diameter 18, 32, 57 and 73 mm by using developed algorithm and experimental data which are consistent with theoretical data. It is shown that the geometric dimensions of the pipe and the presence of the features such as electric welding seam or foreign inclusions in material of the testing object have a significant impact on the dependencies of informative parameters of the signal from the level of clamping force of piezoelectric transducer on the cylindrical surface of the pipe. The obtained results can be used at the improvement of ultrasonic inspection techniques and development of new approaches in material structure testing of the cylindrical long range objects.

Keywords: reflection coefficient, method of multiple reflections, calculation algorithm, attenuation coefficient, piezoelectric transducer, acoustic wave, clamping force, cylindrical long range objects, distant reflections, guided wave testing

INTRODUCTION

In modern industry the cylindrical long range objects such as rod rolling and pipelines for different purposes are widely used which is needed in mandatory inspection both at manufacturing company and during exploitation. For testing of such objects the active methods are basically used using torsional [1–3], rod [4–6], longitudinal [1–3, 7–9], or shear [2, 3, 10, 11] waves thus it is known cases of application of passive methods, in particular, the acoustic emission technique [12]. Among acoustic testing methods of cylindrical long range objects guided wave testing is widespread which have several advantages over classical ultrasound methods of nondestructive testing including an opportunity of rapid long range inspection, absence of necessity in scanning, and testing range of cylindrical long range objects up to 100 meters in the selected direction [13, 14]. Recently many authors are paid much attention to

© Myshkin, Yu. V., Efremov, A. B., 2017

modeling and experiments aimed at the investigation of the influence of external and internal viscoelastic media on the propagation of acoustic waves in pipes of different diameters [14–16].

The implementation of guided wave technique is available using piezoelectric dry coupled transducers [1, 3, 9, 17], magnetostrictive transducers [11, 18, 19] and electromagnetic acoustic (EMA) transducers [20-24] which have advantages: the possibility of testing without any contact with testing object at small gaps, generate any type of wave mode, absence of wear of element design and low absorption of acoustic wave energy by transducer [20, 21, 24, 25]. However, EMA transducers usually have low efficiency of EMA transformation in comparison with piezoelectric transducers and can not be used for testing of non-ferromagnetic materials [24–27].

Guided wave testing is predominantly used in the oil, gas and petroleum industry for the cylindrical long range objects and products from them such as sucker rods [5, 28], oil well tubing and pipes [24, 29, 30], metal cables [31–33], reinforcing bars [34, 35], workpieces for the steel springs [36], rock bolts [37, 38], and etc. Since the products represent the objects of the final length for such objects the technique has been developed and successfully used based on the method of multiple reflections (MMR) which have several advantages [4, 29, 39]:

– increases sensitivity and calculation accuracy of the wave speed and attenuation when analyzing the acoustic signals of distant reflections;

– has high informative value of testing through using additional characteristics of the acoustic signal;

– improves the distance resolution;

– decreases the dead zone through a low quality factor of the signal.

At the implementation of the MMR it is needed to consider the wave attenuation in the testing object and incomplete reflection of the signal on the interface between transducer and the surface of the testing object, called the reflection coefficient, which depend on several factors such as a clamping force of the transducer to the testing object, quality of acoustic coupling, roughness of the surface of the testing object, exact location of the transducer system on the cylindrical surface of the testing object. Reflection coefficient depend on the informative parameters of guided wave testing such as the reflection coefficient from the defects, attenuation of multiple reflection pulses, velocity of the wave propagation, efficiency of EMA and piezoelectric transformations [4–6, 29, 39]. As a rule, the reflection coefficient values may vary within the range from 0 to 1. Decreasing of this value to 0.7 and below there is the absence of growing defect amplitude effect at the distant reflections that leads to low efficiency of the MMR [39].

In this article, the algorithm and program implementation is represented and designed for increasing of the informative value of guided wave testing of the cylindrical long range objects using the MMR in real time during testing allowing, in particular, to compute the reflection coefficient and attenuation coefficient at the distant reflections, to determine probe pulse amplitude and position. There are the results of experiments confirming the efficiency of the algorithm operation on the real data.

APPROACHES USED

It is known, that at the implementation of the MMR a part of the acoustic wave energy is absorbed on the interface between transducer and the surface of the testing object and this physical phenomenon can be described by mathematical model taking into account of equipment parameters, geometric and elastic properties of the testing object, wave attenuation, and interaction with defects. The law of propagation of the rod and torsional waves in the cylindrical long range objects at the implementation of the MMR is known and a series of the multiple reflections is described by the expression [39]:

$$U_n = U_0 \cdot R_e{}^n \cdot e^{-\delta \cdot (x_n - x_0)}, \quad (1)$$

where U_n – echo pulse amplitude from the end of the testing object at the n-th reflection; U_0 – probe pulse amplitude; R_e – reflection coefficient on the interface between transducer and the surface of the testing object; δ – attenuation coefficient of acoustic wave; $x_n = 2 \cdot L \cdot n + x_0$ – position of the n-th reflection, $2\ L\ n$ – traveled distance of acoustic wave at the n-th reflection; x_0 – probe pulse position, $L = C \cdot t$ – length of the testing object, C – propagation velocity of acoustic wave, t – propagation time of acoustic wave.

The problem is to find the reflection coefficient R_e for which the equation (1) on the reflection n at the reflection amplitude U_n and the distance to the reflection x_n has a unique solution. It also follows from the equation (1) that the variables R_e, U_0, and δ are interdependent, therefore, the calculation of their values should be carried out on the different reflections n.

THE CALCULATION ALGORITHM

The solution of the problem can be accomplished by using the bisection method based on the successive approximation to the desired value of the unknown quantity by dividing the search interval into two and calculation of interdependent unknown variables on each iteration.

Input data

As the input data, the peak coordinates of the two pulses reflected from the end of the testing object are used: U_n, U_m – amplitudes of the echo pulses from the end of the testing object at the n-th and m-th reflection respectively, x_n, x_m – propagation distance of acoustic wave to the n-th and m-th reflection respectively $x_n = 2 \cdot L \cdot n + x_0$ and $x_m = 2 \cdot L \cdot m + x_0$, when condition $m > n$ must be satisfied, where n and m – whole numbers.

It is calculated the distance which equal to double size of the length of pipe and corresponding to the space between the two pulses on the distance scale:

$$\Delta x = 2L = \frac{x_m - x_n}{m - n}. \quad (2)$$

Probe pulse position on the x-axis is determined as

$$x_0 = x_n - n \cdot \Delta x. \quad (3)$$

Initial value of attenuation coefficient is introduced and reflection coefficient is calculated for launching the calculation cycle

$$\delta = 0,\ R_{en} = 1,\ R_{em} = \left[\frac{U_m}{U_0}\right]^{\frac{1}{m}},\ R_e = \frac{R_{en} + R_{em}}{2}, \quad (4)$$

where R_{en} – reflection coefficient at the n-th reflection; R_{em} – reflection coefficient at the m-th reflection.

Probe pulse amplitude is calculated by using this data

$$U_0 = \frac{U_n}{R_e{}^n}. \quad (5)$$

Formulas (2)–(5) are used for the calculation one time only and they are needed for launching the main calculation cycle.

Main calculation cycle

The calculation algorithm of the informative parameters of the signal in the main calculation cycle at iteration step *k* looks as follows.

1. Computation R_e at the *n*-th reflection

$$R_{en} = \left[\frac{U_n}{U_0 \cdot e^{-\delta \cdot (x_n - x_0)}} \right]^{\frac{1}{n}}. \tag{6}$$

2. Computation R_e at the *m*-th reflection

$$R_{em} = \left[\frac{U_m}{U_0 \cdot e^{-\delta \cdot (x_m - x_0)}} \right]^{\frac{1}{m}}. \tag{7}$$

3. Calculation of the average value R_e

$$R_e = \frac{R_{en} + R_{em}}{2}. \tag{8}$$

4. Evaluation of the value ΔR_e

$$\Delta R_e = \left| (R_e)_k - (R_e)_{k-1} \right|. \tag{9}$$

5. Calculation of the attenuation coefficient with considering the calculated reflection coefficient R_e

$$\delta = -\frac{\ln\left(\dfrac{U_m}{U_0 \cdot R_e^{\,m}} \right)}{x_m - x_0}. \tag{10}$$

6. Calculation of the probe pulse amplitude with considering the calculated reflection coefficient R_e (formula 8) and attenuation coefficient δ (formula 10)

$$U_0 = \frac{U_n}{R_e^{\,n} \cdot e^{-\delta \cdot (x_n - x_0)}}. \tag{11}$$

The exit from the cycle body is carried out when the condition $\Delta R_e \le 10^{-6}$ is satisfied. Thus, the represented algorithm allows to obtain the values of reflection coefficient R_e, attenuation coefficient δ, probe pulse amplitude U_0 and position x_0 with a specified accuracy.

Implementation of algorithm

The algorithm is implemented as part of program in the software called Prince which is written using high level programming language Object Pascal and designed for equipment management, recording of acoustic signals and the output of main informative parameters of the signal in the real-time, including the values of reflection coefficient, attenuation coefficient, probe pulse amplitude and position on the monitor screen. A scheme of calculation algorithm of the reflection coefficient is provided in Fig. 1 and it includes a data input unit, preliminary calculation unit, result output unit and main cycle body which contains the units of reflection coefficient calculation, error checking, computation of attenuation coefficient and probe pulse amplitude.

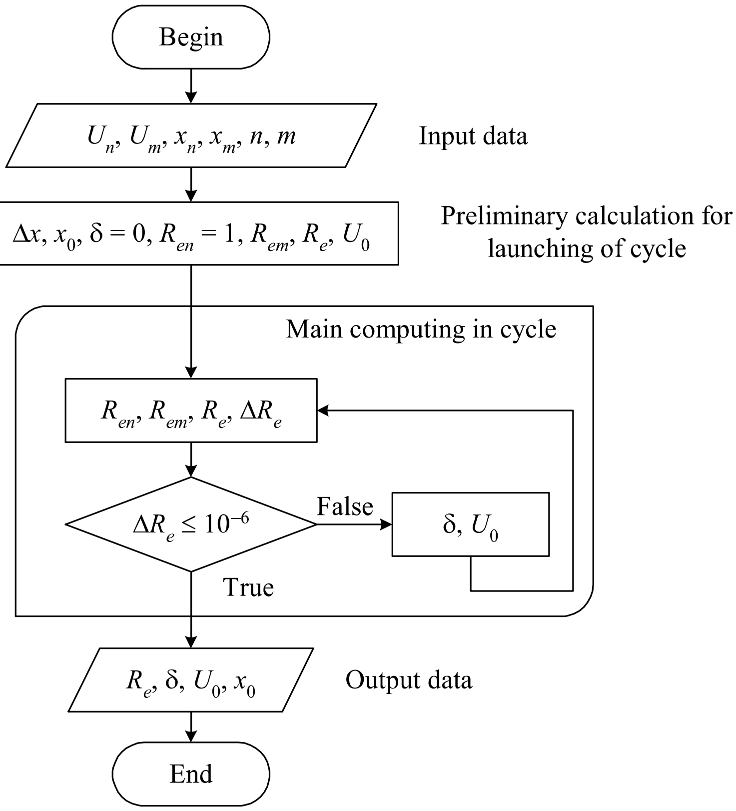

Figure 1. A scheme of the calculation algorithm of the informative parameters of the signal

For instance, the operation of the algorithm on the real data is represented in table 1. As the input data for calculating, the following data are used: $n = 1$, $m = 5$, $U_n = 931.091$ mV, $U_m = 711.914$ mV, $x_n = 2.018$ m, $x_m = 9.630$ m, $C = 3250$ m/s. The output data: $R_e = 0.954193$, $\delta = 0.010744$, $U_0 = 995.710785$ mV, $x_0 = 0.1144$ m.

Table 1. An example of the operation of the algorithm on each iteration

Iteration number k	Reflection coefficient at n-th reflection R_{en}	Reflection coefficient at m-th reflection R_{em}	Average value of reflection coefficient R_e	Attenuation coefficient δ	Probe pulse amplitude U_0 mV	Condition ΔR_e
1	1	0.9477353	0.9738677	0	956.0757988	-
2	0.9738677	0.9427294	0.9582985	0.0086066	987.6548819	0.0155692
3	0.9582985	0.9520905	0.9551945	0.0103168	994.0947786	0.0031040
4	0.955195	0.9539537	0.9545741	0.0106584	995.3877881	0.0006204
5	0.9545741	0.954326	0.9544501	0.0107267	995.6465917	0.0001240
6	0.9544501	0.9544004	0.9544253	0.0107404	995.6983605	0.0000248
7	0.9544253	0.9544153	0.9544203	0.0107431	995.7087146	0.0000050
8	0.9544203	0.9544183	0.9544193	0.0107437	995.7107855	0.0000010

As shown from table 1, for calculating with certain accuracy according to the condition $\Delta R_e \leq 10^{-6}$ the eight iterations are enough to reach of satisfactory solution.

EXPERIMENTAL SETUP

The experiment for verifying the operation of the calculation algorithm of the informative parameters of the signal was prepared and performed. The experimental setup is represented in Fig. 2 described in [40] and consists of two EMA transducers, piezoelectric transducer, probe pulse generator, control block with preamplifier, analog-digital converter board embedded in personal computer. EMA transducers are located on the cylindrical surface of the pipe at the diametrically opposite sides near the pipe end and piezoelectric transducer is located in the middle between two EMA transducers on the cylindrical surface of pipe as well. The pipes with length 950 mm, diameter 18, 32, 57, 73 mm and wall thickness 3, 4.2, 5, 5.5 mm respectively are used in the experiment and pipe with diameter 18 mm has electric welding seam along the entire length of pipe.

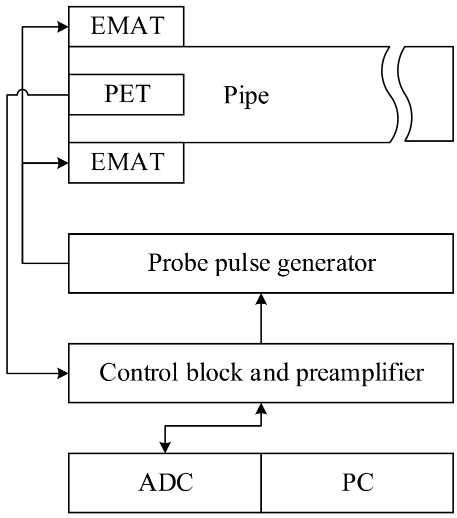

Figure 2. A scheme of the experimental setup, EMAT – electromagnetic-acoustic transducer, PET – piezoelectric transducer, ADC – analog-digital converter, PC – personal computer

The echo signal is the measurement result (Fig. 3) obtained by using the software Prince and represented the series of echo pulses of multiple reflections from the opposite ends of the pipe. For example, in figure 3 the echo signals are illustrated for pipe with diameter 18 mm under one of minimum clamping force and pipe with diameter 57 mm under maximum clamping force. From the presented echo signals it can be concluded that acoustic wave attenuation, acoustic noise level and amplitude of unwanted types of wave modes for pipe with diameter 18 mm is higher than for pipe with diameter 57 mm, it can be explained the presence of electric welding seam along the pipe.

RESULTS AND DISCUSSION

Calculated dependencies of reflection coefficient, attenuation coefficient and probe pulse amplitude from the wave propagation distance for the pipe with diameter 18 mm and 57 mm are given in Fig. 4. The following graphs for the pipe with diameter 18 mm (Fig. 4 a, c, e) demonstrate the insignificant nonlinear dependence of reflection coefficient (Fig. 4 a) from the wave propagation distance the cause of which can be high amplitudes of acoustic noise and unwanted types of wave modes due to structural and geometrical features of the pipe as well as the presence of electric welding seam along the testing object.

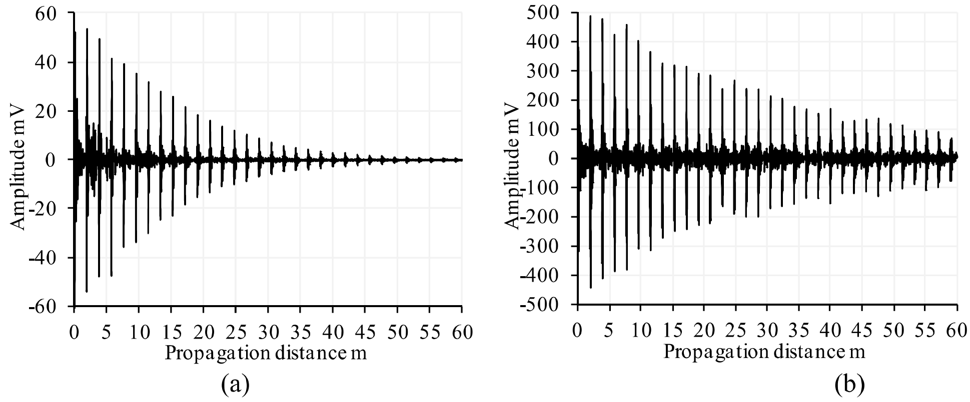

Figure 3. Experimental signals of the series of echo pulses of multiple reflections obtained on the pipes with diameter 18 mm (a) and 57 mm (b)

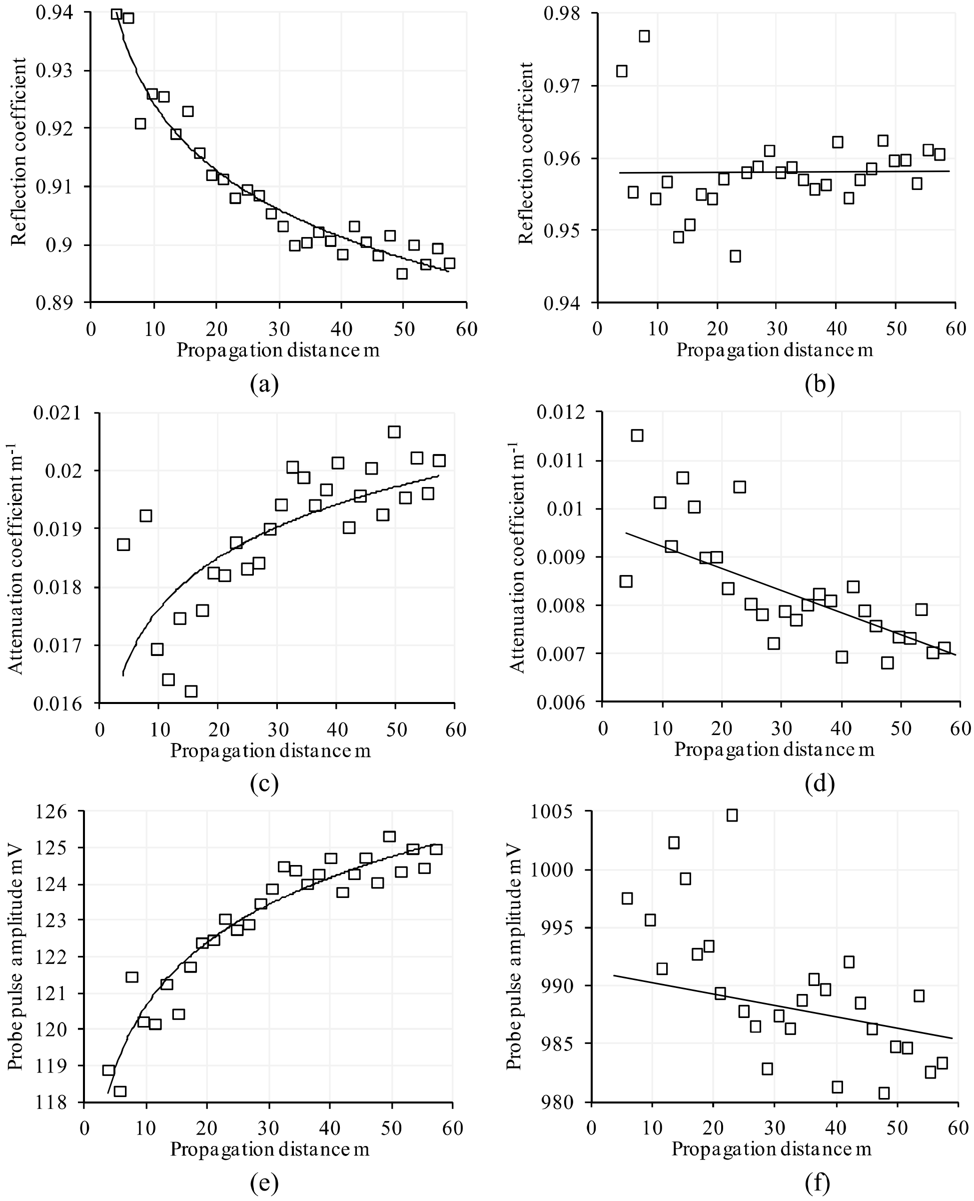

Figure 4. Dependencies of calculated reflection coefficient (a, b), attenuation coefficient (c, d), and probe pulse amplitude (e, f) from the wave propagation distance at the multiple reflections in pipe with diameter 32 mm (a, c, e) and 73 mm (b, d, e)

Main values of attenuation coefficient are within the range 0.016÷0.021 for pipe with diameter 18 mm (Fig. 4 c) and 0.006÷0.012 for pipe with diameter 57 mm (Fig. 4 d). Since the attenuation coefficient is a constant value in defined medium then the average value of attenuation coefficient at the $5^{th} – 8^{th}$ reflection is taken as a constant where unwanted types of wave modes and acoustic noise amplitudes have insignificant influence. Using such approach the calculated attenuation coefficient for pipe with diameter 18, 32, 57, 73 mm is amounted 0.018, 0.024, 0.009, 0.016 m^{-1} respectively.

For comparison of the calculated results the definitions of graphs are accepted on the evaluation of clamping force which carried out the amplitude of the first echo pulse from the opposite end of the pipe (first reflection). Generalized dependencies of average values of reflection coefficient from the first echo pulse amplitude from pipe end for different diameters are represented in Fig. 5. Reflection coefficient for pipe with the smallest diameter 18 mm varies widely from 0.78 to 0.93. However, the variation range of reflection coefficient for pipes with large diameters 32, 57, and 73 mm varies within a range 0.04÷0.08 (0.84÷0.92, 0.93÷0.97, 0.95÷1 for pipe with diameter 32, 73, and 57 mm respectively). Thus, reflection coefficient at the amplitude 500 mV of the first echo pulse from the opposite end of the pipe for pipes with diameters 18, 32, 57, and 73 mm is amounted 0.82, 0.86, 0.97, and 0.94 respectively.

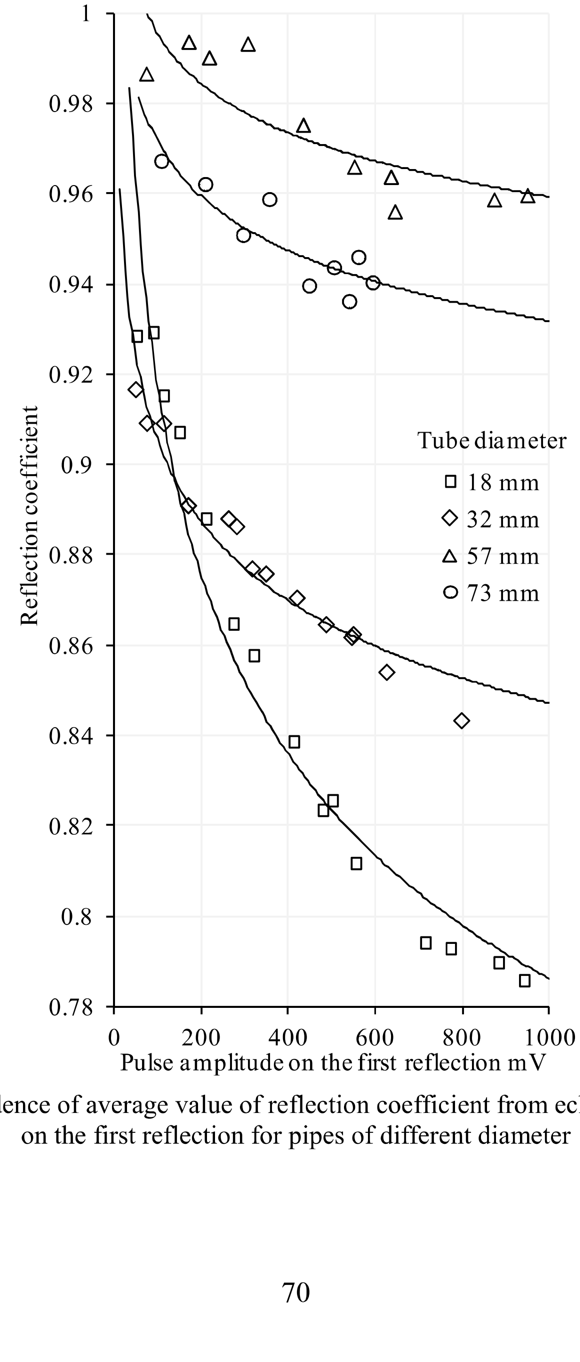

Figure 5. Dependence of average value of reflection coefficient from echo pulse amplitude on the first reflection for pipes of different diameter

General decreasing dependence of reflection coefficient from the first echo pulse amplitude from the opposite end of the pipe is observed on the graphs (Fig. 5). However, this dependence is most pronounced for pipe with diameter 18 mm that can be related with presence of electric welding seam which has a structure differing from main material structure of pipe. Therefore, it can be assumed that the presence of structural inhomogeneity of material in the testing object leads to significant changes of the reflection coefficient at the different clamping force of piezoelectric transducer to the cylindrical surface of pipe. Hence, this approach can be used for development of the technique of guided wave testing for the evaluation of the material structure and the presence of foreign inclusions in pipes with different diameters.

CONCLUSIONS

Thus, according to the results of the developed calculation algorithm of the informative parameters of the signal and experimental investigations at the implementation of the method of multiple reflections it is possible to make the following conclusions:

– presented algorithm allows to obtain with high accuracy in real-time of reflection coefficient (absolute error of the calculated values of reflection coefficient for pipe with diameter 57 mm and 73 mm is amounted 0.02), attenuation coefficient, probe pulse amplitude and position;

– calculated values of reflection coefficient (from 0.77 to 0.99) by using algorithm on the real testing object are consistent with the theoretical data;

– the presence of acoustic noise and unwanted types of wave modes does not have significant influence on the calculation results;

– with increasing the clamping force of piezoelectric transducer to the cylindrical surface of the pipe the reflection coefficient slightly decreases;

– the reflection coefficient has a nonlinear dependence in pipes of small diameters at the presence of foreign inclusions.

The results of the work can be used for the improvement of existing techniques of guided wave testing as well as for the development of approaches in the evaluation of material structure of cylindrical long range objects based on detection of dependence of reflection coefficient from clamping force of piezoelectric transducer on the pipe surface.

ACKNOWLEDGMENTS

This work was supported by the Russian Scientific Foundation, project no. 15-19-00051.

REFERENCES

1. Alleyne, D. N., Vogt, T., & Cawley, P. (2009). The choice of torsional or longitudinal excitation in guided wave pipe inspection. *Insight – Non-Destructive Testing and Condition Monitoring, 51*(7), 373–377. doi:10.1784/insi.2009.51.7.373
2. Mohr, W., & Holler, P. (1976). On inspection of thin-walled tubes for transverse and longitudinal flaws by guided ultrasonic waves. *IEEE Transactions on Sonics and Ultrasonics, 23*(5), 369–374. doi:10.1109/t-su.1976.30893
3. Silk, M., & Bainton, K. (1979). The propagation in metal tubing of ultrasonic wave modes equivalent to Lamb waves. *Ultrasonics, 17*(1), 11–19. doi:10.1016/0041-624x(79)90006-4
4. Budenkov, G. A., Nedzvetskaya, O. V., Budenkov, B. A., Lebedeva, T. N., & Zlobin, D. V. (2004). Acoustic nondestructive testing of rods using multiple reflections. *Russian Journal of Nondestructive Testing*, *40*(8), 541–544. doi:10.1007/s11181-005-0007-y

5. Budenkov, G. A., Nedzvetskaya, O. V., Zlobin, D. V., & Lebedeva, T. N. (2004). The application efficiency of rod and torsional waves for checking rod-shaped roll stock. *Russian Journal of Nondestructive Testing, 40*(3), 147–151. doi:10.1023/b:runt.0000040171.56679.6b
6. Budenkov, G. A., & Nedzvetskaya, O. V. (2004). Principal regularities of Pochhammer-wave interaction with defects. *Russian Journal of Nondestructive Testing, 40*(2), 99–108. doi:10.1023/b:runt.0000036552.46582.a0
7. Alleyne, D. N., & Cawley, P. (1996). The excitation of Lamb waves in pipes using dry-coupled piezoelectric transducers. *Journal of Nondestructive Evaluation, 15*(1), 11–20. doi:10.1007/bf00733822
8. Wang, T., Yang, C., Ye, L., Spray, D., & Xiang, Y. (2014). Evaluation of guided wave propagation in steel pipes. *Recent Advances in Structural Integrity Analysis – Proceedings of the International Congress (APCF/SIF-2014)*, 255–260. doi:10.1533/9780081002254.255
9. Lowe, P., Sanderson, R., Pedram, S., Boulgouris, N., & Mudge, P. (2015). Inspection of pipelines using the first longitudinal guided wave mode. *Physics Procedia, 70*, 338–342. doi:10.1016/j.phpro.2015.08.079
10. Fateri, S., Lowe, P. S., Engineer, B., & Boulgouris, N. V. (2015). Investigation of ultrasonic guided waves interacting with piezoelectric transducers. *IEEE Sensors Journal, 15*(8), 4319–4328. doi:10.1109/jsen.2015.2414874
11. Xu, J., Wu, X., Kong, D., & Sun, P. (2015). A guided wave sensor based on the inverse magnetostrictive effect for distinguishing symmetric from asymmetric features in pipes. *Sensors, 15*(3), 5151–5162. doi:10.3390/s150305151
12. Budenkov, G. A., Nedzvetskaya, O. V., Sergeev, V. N., & Zlobin, D. V. (2000). Potentialities of acoustic emission technique for inspection of main pipelines. *Russian Journal of Nondestructive Testing, 36*(2), 97–102. doi:10.1007/bf02759403
13. Cawley, P. (2003). Practical long range guided wave inspection – Managing Complexity. *AIP Conference Proceedings, 61*(1), 66–74. doi:10.1063/1.1570116
14. Leinov, E., Lowe, M. J., & Cawley, P. (2015). Investigation of guided wave propagation and attenuation in pipe buried in sand. *Journal of Sound and Vibration, 347*, 96–114. doi:10.1016/j.jsv.2015.02.036
15. Murav'eva, O. V., Len'kov, S. V., & Myshkin, Y. V. (2016). Factors affecting attenuation of torsional waves in pipes loaded on contact viscoelastic media. *Russian Journal of Nondestructive Testing, 52*(9), 485–491. doi:10.1134/s1061830916090035
16. Na, W., & Yoon, H. (2007). Wave-attenuation estimation in fluid-filled steel pipes: The first longitudinal guided wave mode. *Russian Journal of Nondestructive Testing, 43*(8), 549–554. doi:10.1134/s1061830907080074
17. Zhou, W., Yuan, F., & Shi, T. (2016). Guided torsional wave generation of a linear in-plane shear piezoelectric array in metallic pipes. *Ultrasonics, 65*, 69–77. doi:10.1016/j.ultras.2015.10.021
18. Cheong, Y. M., Kim, S., & Jung, H. K. (2007). Application of magnetostrictive transducer for the long-range guided wave inspection. *The Mechanical Behavior of Materials X, 345–346,* 1295–1298. doi:10.4028/www.scientific.net/KEM.345-346.1295
19. Guo, P., Li, H., Tian, Z., & Xu, H. (2015). Guided wave damage detection in power-plant-tubes by using magnetostrictive transducer arrays. *Pressure Vessels and Piping Conference. Volume 6A: Materials and Fabrication*. Boston, USA: ASME. doi:10.1115/pvp2015-45845
20. Huang, S., & Wang, S. (2016). The electromagnetic ultrasonic guided wave testing. In Huang, S., & Wang, S. (Eds.) *New Technologies in Electromagnetic Non-destructive Testing*. Singapore: Springer. doi:10.1007/978-981-10-0578-7_1
21. Murav'eva, O. V., Len'kov, S. V., & Murashov, S. A. (2016). Torsional waves excited by electromagnetic–acoustic transducers during guided-wave acoustic inspection of pipelines. *Acoustical Physics, 62*(1), 117–124. doi:10.1134/s1063771015060093
22. Murayama, R. (2016). A new guide wave inspection system using three polarized transverse wave EMATs without any couplant. *Journal of Sensor Technology, 6*(4), 110–121. doi:10.4236/jst.2016.64009

23. Furusawa, A., Kojima, F., & Morikawa, A. (2015). Mode control of guided wave in magnetic hollow cylinder using electromagnetic acoustic transducer array. *Nuclear Engineering and Technology, 47*(2), 196–203. doi:10.1016/j.net.2014.12.007

24. Hirao, M., & Ogi, H. (2003). EMATs for Science and Industry. Noncontacting Ultrasonic Measurements. Boston, USA: Springer. doi:10.1007/978-1-4757-3743-1

25. Cheng, J., & Bond, L. J. (2015). Assessment of ultrasonic NDT methods for high speed rail inspection. *AIP Conference Proceedings*, *1650*, 605–614. doi:10.1063/1.4914660

26. Mikhailov, A. V., Gobov, Y. L., Smorodinskii, Y. G., & Shcherbinin, S. V. (2015). An electromagnetic–acoustic transducer with pulsed biasing. *Russian Journal of Nondestructive Testing, 51*(8), 467–475. doi:10.1134/s1061830915080069

27. Thring, C., Fan, Y., & Edwards, R. (2016). Focused Rayleigh wave EMAT for characterisation of surface-breaking defects. *NDT & E International, 81*, 20–27. doi:10.1016/j.ndteint.2016.03.002

28. Brook, M. V., & Wiley InterScience (Online service). (2012). Technique development and probe design for cylindrical rod inspection. In *Ultrasonic inspection technology development and search unit design: Examples of practical applications* (pp. 135–162). Hoboken, USA: John Wiley & Sons, Inc. doi:10.1002/9781118104781.ch7

29. Budenkov, G. A., Nedzvetskaya, O. V., Zlobin, D. V., & Murashov, S. A. (2006). Interaction of torsion waves with longitudinal cracks in tubes. *Russian Journal of Nondestructive Testing, 42*(6), 392–397. doi:10.1134/s1061830906060064

30. Sabhnani, R. M., Humphrey, V., Zaghari, B., & Moshrefi-Torbati, M. (2015). Fault detection in small diameter pipes using ultrasonic guided wave technology. *Sensors and Smart Structures Technologies for Civil, Mechanical, and Aerospace Systems 2015, 9435*, 1–13. doi:10.1117/12.2085494

31. Baltazar, A., Hernandez-Salazar, C. D., & Manzanares-Martinez, B. (2010). Study of wave propagation in a multiwire cable to determine structural damage. *NDT & E International, 43*(8), 726–732. doi:10.1016/j.ndteint.2010.08.007

32. Farhidzadeh, A., & Salamone, S. (2015). Reference-free corrosion damage diagnosis in steel strands using guided ultrasonic waves. *Ultrasonics, 57*, 198–208. doi:10.1016/j.ultras.2014.11.011

33. Legg, M., Yücel, M. K., Kappatos, V., Selcuk, C., & Gan, T. (2015). Increased range of ultrasonic guided wave testing of overhead transmission line cables using dispersion compensation. *Ultrasonics, 62*, 35–45. doi:10.1016/j.ultras.2015.04.009

34. Karayannis, C. G., Chalioris, C. E., Angeli, G. M., Papadopoulos, N. A., Favvata, M. J., & Providakis, C. P. (2016). Experimental damage evaluation of reinforced concrete steel bars using piezoelectric sensors. *Construction and Building Materials, 105*, 227–244. doi:10.1016/j.conbuildmat.2015.12.019

35. Sharma, S., & Mukherjee, A. (2010). Longitudinal guided waves for monitoring chloride corrosion in reinforcing bars in concrete. *Structural Health Monitoring, 9*(6), 555–567. doi:10.1177/1475921710365415

36. Murav'ev, V. V., Murav'eva, O. V., Strizhak, V. A., Pryakhin, A. V., & Fokeeva, E. N. (2014). An analysis of the comparative reliability of acoustic testing methods of bar stock from spring steels. *Russian Journal of Nondestructive Testing, 50*(8), 435–442. doi:10.1134/s1061830914080063

37. Stepinski, T., & Mattson, K. (2015). Instrument for rock bolt inspection by means of ultrasound. *2015 IEEE International Ultrasonics Symposium (IUS)*. Taipei, Taiwan: IEEE. doi:10.1109/ultsym.2015.0343

38. Sun, B., Zeng, S., Guo, S., & Yang, C. (2015). Variation characteristics of stress wave speed for anchorage system under instantaneous excitation. *Geotechnical and Geological Engineering, 33*(3), 751–757. doi:10.1007/s10706-015-9846-z

39. Murav'eva, O. V., & Zlobin, D. V. (2013). The acoustic path in the method of multiple reflections during nondestructive testing of linearly extended objects. *Russian Journal of Nondestructive Testing, 49*(2), 93–99. doi:10.1134/s1061830913020058

40. Murav'eva, O. V., Len'kov, S. V., Murav'ev, V. V., Myshkin, Y. V., & Murashov, S. A. (2016). Factors that affect the excitation effectiveness of torsional waves during waveguide inspection of pipes. *Russian Journal of Nondestructive Testing, 52*(2), 78–84. doi:10.1134/s1061830916020066